This is the peer reviewed version of the following article: ***Journal of the American Ceramic Society*** 89, 202-209 (2006), which has been published in final form at http://onlinelibrary.wiley.com/doi/10.1111/j.1551-2916.2005.00675.x/full. This article may be used for non-commercial purposes in accordance With Wiley Terms and Conditions for self-archiving.

Influence of Cation Order on the Electric Field-Induced Phase Transition in $Pb(Mg_{1/3}Nb_{2/3})O_3$-Based Relaxor Ferroelectrics

Xiaohui Zhao, Weiguo Qu, Hui He, Naratip Vittayakorn,[†] and Xiaoli Tan[*,¶]

Department of Materials Science and Engineering, Iowa State University, Ames, Iowa 50011

The effect of cation ordering on the electric field-induced relaxor to normal ferroelectric phase transition in $Pb(Mg_{1/3}Nb_{2/3})O_3$-based ceramics was investigated. Both A-site, La-doping, and B-site, Sc-doping, were found to enhance the chemical ordering in these relaxor ceramics. However, the enhanced chemical orderings showed different impacts on the dielectric and ferroelectric properties in these perovskite materials. The 5% La-doping was observed to shift the dielectric maximum temperature (T_{max}) to a significantly lower temperature and suppress the electric field-induced transition to a ferroelectric phase. In contrast, the 5% and 10% Sc-doping showed little effect on T_{max} but strengthened the ferroelectric coupling. The difference is discussed on the basis of cation size and charge imbalance. An electric field-temperature phase diagram is also proposed for the $0.90Pb(Mg_{1/3}Nb_{2/3})O_3$–$0.10Pb(Sc_{1/2}Nb_{1/2})O_3$ based on its history dependence of the electric field-induced phase transition.

This work was supported by the National Science Foundation through the CAREER grant DMR-0346819.

[†]Currently at Department of Chemistry, King Mongkut's Institute of Technology, Thailand.

[*]Member, American Ceramic Society.

[¶]Author to whom correspondence should be addressed.

I. Introduction

Complex perovskite $Pb(Mg_{1/3}Nb_{2/3})O_3$ (PMN)-based relaxor ferroelectrics have been extensively studied for several decades due to their unique dielectric, ferroelectric, and electrostrictive properties.[1-3] The characteristic diffuse phase transition was initially suggested to be caused by microscale compositional fluctuations.[1] Such chemical heterogeneities were later confirmed by transmission electron microscopy investigations, taking the form of nanometer scale B-site cation ordered domains.[4-7] Coupling to this chemical ordering, electrical dipole ordering also exists in the form of polar nanoregions in these relaxor ferroelectrics and these nanoscale polar domains persist well above the diffuse phase transition temperature T_{max}.[8]

The B-site 1:1 cation ordered domains in PMN are highly stable against extended thermal annealing.[5-7] Two models have been proposed to interpret the nonstoichiometric chemical ordering in these PMN-based 1:2 complex perovskites. One is the "space charge model" where Mg and Nb occupy the {111} plane alternatively.[2-6] This model suggests that the cation ordered domains carry negative space charges. The disordered matrix is Nb-rich and hence positively charged. The space charge prevents the growth of the cation ordered domains during thermal annealing. The other B-site cation ordering model is the recently proposed "random site model" and seems to have gained more experimental support.[7,9-14] In this model, every other {111} plane of the B-site sublattice is occupied solely by Nb cations. The rest {111} planes of the B-site sublattice are occupied randomly by Mg and Nb cations at a ratio of 2:1. This model preserves the charge neutrality of the cation ordered domains and the growth of the chemically ordered domains is limited by kinetics considerations.[9-12]

The electrical dipole ordered nanoregions in PMN are structurally distorted along the <111> directions and the polar axis of these nanodomains is randomly fluctuating among the

eight equivalent directions.[2,3] External electric fields can strengthen the dipole ordering and grow the polar nanoregions into large domains.[15-24] This process corresponds to a first order relaxor to normal ferroelectric phase transition. Presumably, the nanoscale cation ordering should have strong interactions with the nanoscale dipole ordering and the cation ordering would not be affected by external electric fields. However, the particular information on such interactions is still lacking and the effect of cation order on the electric field-induced polar nanoregion coarsening in the PMN-based relaxor ferroelectrics is still not clear.[12,25,26] The present work investigates the influence of chemical ordering on the field-induced phase transition in La-doped and Sc-doped PMN ceramics.

II. Experimental Procedure

$Pb_{1-x}La_x(Mg_{(1+x)/3}Nb_{(2-x)/3})O_3$ (x = 0.05, abbreviated as PLMN5 hereafter) and $(1-x)Pb(Mg_{1/3}Nb_{2/3})O_3$–$xPb(Sc_{1/2}Nb_{1/2})O_3$ (x = 0.05, 0.10, abbreviated as PSMN5 and PSMN10 hereafter, respectively) ceramics were prepared via the columbite method developed by Swartz and Shrout.[27] The starting materials used in this work were commercially available high purity (better than 99.9 wt.%) PbO, MgO, Nb_2O_5, La_2O_3, and Sc_2O_3 powders. After vibratory milling in isopropyl alcohol for 6 hours and subsequent drying, the well-mixed stoichiometric powders of B-site oxides were calcined at 1100°C for 6 hours. The calcined powders were then mixed with La_2O_3 and/or PbO powders, milled for 6 hours, and calcined at 900°C for 4 hours to form phase pure perovskite powders. Pressed cylinders, 15 mm in diameter by 20 mm thick, were formed by cold-isostatic pressing at 350 MPa. The preformed pellets were then hot pressed in an Al_2O_3 die at 1150°C for 2 hours in air. Afterward, the thin slices from the hot pressed piece were buried in PMN powder and annealed at 1250°C for 1 hour. With an oxygen flow rate about 1000 ml/min, a

second annealing was then carried out at 900°C for 6 hours in an atmosphere containing excess PbO. A heating/cooling ramp rate of 300°C/hour was generally used for these thermal processes. One slice of the $0.90Pb(Mg_{1/3}Nb_{2/3})O_3$–$0.10Pb(Sc_{1/2}Nb_{1/2})O_3$ ceramic was further thermally treated at 1250°C for 3 hours and slowly cooled to 900°C at the rate of 10°C/hour. This slow-cooled sample is referred to as "PSMN10 ordered" ceramic hereafter.

The density of these ceramics was measured by the Archimedes' method and their grain size was examined by scanning electron microscopy (SEM). The surface layers of the annealed slices were removed by mechanical grounding and x-ray diffraction was used to check the phase purity and the cation ordering. The cation ordering was also examined by dark field imaging in a transmission electron microscope (TEM). Dielectric characterization was performed with an LCR meter (HP-4284A, Hewlett-Packard) in conjunction with an environmental chamber (9023, Delta Design). A heating/cooling rate of 3°C/min was used during the measurement. Electric field-induced phase transition was then evaluated by the thermal depolarization measurement with a picoammeter (Model 484, Keithley) and the polarization hysteresis measurement with a standardized ferroelectric test system (RT-66A, Radiant technologies).

III. Results and Discussion

Density measurement indicates that all four ceramics have relative densities in the range of 95~98%. SEM examination confirms the high relative density and also reveals the grain size in these ceramics. As shown in Fig. 1, PSMN5, PSMN10 and PLMN5 have fine grains (average grain size <5μm) while the "PSMN10 ordered" ceramic has larger grains (average grain size ~8μm). X-ray diffraction confirms that phase pure perovskite was formed in all compositions. Fig. 2 shows the diffraction spectrum with 2θ from 15° to 25°. The appearance of the (½ ½ ½)

peak in the "PSMN10 ordered" and PLMN5 ceramics is indicative of an enhanced ordering on the B-site cation sublattice. It has been reported before that doping by La at A-site and Sc at B-site are both capable of coarsening B-site cation ordering domains in PMN.[5,11,12,28] It is evident from Fig. 2 that the effect of Sc-doping on enhancing the chemical ordering is more moderate compared to that of the La-doping. The strong cation ordering that is detectable by x-ray diffraction only developed in the slowly cooled PSMN10 sample (the "PSMN10 ordered" ceramic). The ordering parameter α, evaluated according to the common procedure used in literature,[11] for the "PSMN10 ordered" and PLMN5 ceramic is 0.9 and 0.7, respectively. The strong 1:1 cation ordering in these two ceramics is further confirmed by TEM analysis. Figure 3 shows the dark field images formed with the (½ ½ ½) superlattice spot in the <110>-zone axis electron diffraction pattern. Cation ordering domains on the order of 100 nm were observed in both ceramics, with those in the "PSMN10 ordered" ceramic slightly larger than those in the PLMN5 ceramic.

PSMN5, PSMN10 and PLMN5 have similar grain size while the "PSMN10 ordered" ceramic has larger grains. The difference in grain size may contribute to their different dielectric properties. However, it is believed that the cation ordering plays a decisive role in dictating the dielectric and ferroelectric properties in these PMN-based relaxor ferroelectrics. The argument is made based on the experimental observations on undoped PMN. In this prototype relaxor ferroelectric ceramic, extended high temperature annealing presumably develops larger grains. However, no noticeable change in dielectric properties was observed primarily due to the fact that the degree of cation ordering was not altered during the annealing.[5-7] The following discussion is, therefore, focused on the effect of cation ordering on the dielectric and ferroelectric properties.

The dielectric properties of these ceramics are shown in Fig. 4. The relative permittivity of all samples exhibits characteristics of a typical relaxor, namely a broad peak and a strong frequency dispersion. The maximum dielectric loss occurs in the vicinity of T_{max} and is in the range of 0.10~0.12 for all four ceramics. In PLMN5, the relative permittivity was dramatically suppressed and the temperature at dielectric maxima T_{max} shifted considerably to a lower temperature (-80°C at 1 kHz). The results are consistent with previous studies.[5,28] The shift in T_{max} was suggested to be caused by the smaller size of La^{3+} cations and the deviation of Mg:Nb ratio from 1:2.[5] In contrast, little change in T_{max} was noted in both PSMN5 and PSMN10. Increasing Sc-dopants from 5% to 10% led to an increase in T_{max} about 4°C at 1kHz and a decrease in relative permittivity. At the same Sc-doping level of 10%, it is interesting to notice that the T_{max} of the "PSMN10 ordered" ceramic was about 9°C lower at 1kHz than that of the PSMN10 ceramic, together with a further decrease in the permittivity. In these Sc-doped PMN ceramics, the degree of chemical ordering presumably increases in the sequence of PSMN5, PSMN10, and "PSMN10 ordered". Results from Fig. 4 indicate that such an increase in cation order leads to a decrease in the relative permittivity. In this respect, the PLMN5 follows the same trend; it has strong chemical order but weak dielectric response.

It is known that several ferroelectric states exist in PMN-based relaxor ferroelectrics under different temperature/electric field conditions.[15-24] One of the most important parameters that delineate these states is the thermal depolarization temperature T_{d0} under the "zero-field-heating after field-cooling" condition. The temperature T_{d0} is typically several tens of degrees lower than the diffuse phase transition temperature T_{max} and marks a real phase transition. Therefore, T_{d0} has been considered as an intrinsic material property for relaxor ceramics.[22] Typically, T_{d0} is measured by monitoring the thermal depolarization current of a field cooled

sample. Figure 5 shows the results of such measurement on the four hot-pressed ceramics. The PSMN5, PSMN10 and "PSMN10 ordered" ceramics were field-cooled with 10 kV/cm down to -150°C and the PLMN5 ceramic was cooled with the same field down to -185°C before the measurement. Again, the PLMN5 ceramic showed a completely different behavior from that of Sc-doped ceramics. A very weak and broad current peak was detected at -155°C during heating. In sharp contrast to this, strong peaks were detected in all three Sc-doped ceramics. The thermal depolarization process in both PSMN5 and PSMN10 occurred in a relatively wide temperature range compared to that in the "PSMN10 ordered" ceramic. The measured T_{d0} values are -66°C, -64°C, and -51°C for PSMN5, PSMN10, and "PSMN10 ordered", respectively, and are listed in Table 1 with other dielectric properties.

It is worth comparing the T_{max} and T_{d0} of PSMN10 with those of "PSMN10 ordered". Slow cooling enhanced the cation order in the "PSMN10 ordered" ceramic. The strengthened chemical ordering increased the T_{d0} from -64°C to -51°C and decreased the T_{max} from -8°C to -17°C. In other words, the enhanced chemical ordering in "PSMN10 ordered" reduced the gap between T_{d0} and T_{max}. It should be pointed out that T_{d0} and T_{max} converge to the Curie temperature T_c in normal ferroelectrics with long range dipole order. Therefore, increasing the lengthscale of the chemical ordering in Sc-doped PMN leads to an increase in the lengthscale of the electric dipole order as well.[12]

The electric field-induced relaxor to normal ferroelectric phase transition was characterized by the polarization hysteresis measurement at temperatures below T_{max}. The result for PLMN5 at 30kV/cm is shown in Fig. 6. It is evident that a normal ferroelectric phase could hardly be forced to form by external fields. Consistent with the thermal depolarization measurement, very low remanent polarization P_r and saturation polarization P_s was measured.

The A-site La-doping shifted both T_{max} and T_{d0} significantly down to lower temperatures. In general, a normal ferroelectric phase could be induced by electric fields in relaxor ferroelectrics at temperatures in the vicinity of T_{d0}. The polarization hysteresis loop did open up slightly at -150°C, which is close to T_{d0} (-155°C). However, it seems that the electrical dipoles in the random polar nanodomains are frozen and cannot be aligned by external electric fields at such low temperatures.

In contrast, the polarization hysteresis measurements on PSMN5, PSMN10, and "PSMN10 ordered" showed a very well defined relaxor to normal ferroelectric phase transition, as demonstrated in Fig. 7. It is clear that square hysteresis loops, indicating the presence of a normal ferroelectric phase, can be induced by external electric fields at temperatures around T_{d0}. The enhanced chemical ordering in Sc-doped PMN at least preserves, if not enhances, the electric field-induced relaxor to normal ferroelectric phase transition.

Ferroelectric properties, the remanent polarization P_r and the coercive field E_c, were measured from the hysteresis loops and are plotted in Fig. 8. Sharp contrast is seen again between the PLMN5 and the three Sc-doped ceramics. The PLMN5 ceramic showed a minimal P_r and a low E_c. The three Sc-doped ceramics showed a peak in P_r at -120°C, indicating the optimum temperature to align most of the electrical dipoles. A high P_r (>15μC/cm^2) was observed to persist at -50°C in the slow cooled "PSMN10 ordered" ceramic. At -20°C, which is close to their T_{max}, P_r was found to diminish for all three Sc-doped ceramics. A monotonic decrease in the coercive field E_c with increasing temperature is shown in Fig. 8(b). This indicates a higher resistance for the polarization switching at lower temperatures, consistent with previous observations.[19-22] In comparison to PSMN5 and PSMN10, "PSMN10 ordered" shows a higher E_c

at temperatures below T_{d0}. This could be a result of the larger polar nanodomains in this ceramic, since a larger polar domain needs a higher field to switch its polarization.

Strong dependence of the field-induced phase transition in undoped PMN upon temperature/electric field history has been previously reported.[19-23] Such history dependence was also examined in the PSMN10 and the "PSMN10 ordered" ceramics with the polarization hysteresis measurement. Three temperature/electric field conditions were used and compared. In the first condition, the sample was initially heated to 150°C and held for one hour and then zero-field cooled down to the desired temperature for the hysteresis measurement. At this temperature, the measurement was performed at electric fields in the sequence of 5, 10, 15, 20, 30, and 40 kV/cm, respectively. This condition is referred to as "zero-field-cooled" condition in the following. In the second condition, the hysteresis measurement was carried out right after the measurement under the first condition at the same temperatures at the same field sequence. The second condition is referred to as "poled" condition in the following discussion. In the third condition, the sample was initially heated to 150°C for one hour and then zero-field cooled to -150°C. At -150°C, a ferroelectric phase was induced by applying a full cycle of AC field of 40kV/cm. Then the sample was zero-field heated to desired temperatures for polarization hysteresis measurement at fields in the sequence of 5, 10, 15, 20, 30 and 40 kV/cm.

Identical polarization hysteresis loops were observed under the second and the third conditions at all field levels in both the PSMN10 and the "PSMN10 ordered" ceramics. However, a significant difference was noticed in the hysteresis loops measured under the first condition when the field was below a critical level. Figure 9 shows the comparison between the "zero-field cooled" and the "poled" conditions in the PSMN10 ceramic. At -120°C, a lower P_r was observed under the "poled" condition at field levels of 5, 10, and 15 kV/cm. However, the situation was

reversed at 20kV/cm where a higher P_r was measured under the "poled" condition, as shown in Fig. 9 (a) and (b). Identical hysteresis loops under these two conditions were observed at 30 and 40 kV/cm field levels at this temperature. The electric field level marking the different appearance of the hysteresis loops (taken as 25 kV/cm for this temperature) is termed the critical electric field in discussion followed. At -100°C and -80°C, a higher P_r was measured under the "poled" condition at fields below the critical electric field, as shown in Fig. 9 (c) and (d). The critical field was roughly determined to be 12.5kV/cm at -100°C and 7.5kV/cm at -80°C.

Similar plots for the "PSMN10 ordered" ceramic under the "zero-field cooled" and "poled" conditions are shown in Fig. 10. Again, a higher P_r was measured under the "poled" condition at fields below a critical electric field. At -120°C and -80°C, a significant difference in P_r was noticed. The critical electric field was determined as 25kV/cm at -120°C, 12.5kV/cm at -80°C, and 7.5kV/cm at -50°C, respectively.

The critical field can be considered as a threshold field for transforming the relaxor ferroelectric state to the normal ferroelectric state. This is best illustrated by the hysteresis loops displayed in Fig. 9(d), Fig. 10(a), and Fig. 10(b). The hysteresis loops in these figures under the "poled" condition are asymmetric, with one corner sharp and one round. Such loops strongly resemble those in poled normal ferroelectric ceramics, such as piezoelectric lead zirconate titanate ceramics. According to previous studies on undoped PMN and $Pb(Zn_{1/3}Nb_{2/3})O_3$,[22,29] the PSMN10 and the "PSMN ordered" ceramics are believed to be at a "frozen macrodomain" state at electric fields below the critical electric field and at a "normal ferroelectric" state at fields above the critical levels. Therefore, an electric field vs. temperature phase diagram can be constructed for the PSMN10 and the "PSMN10 ordered" ceramics based on the values of the critical electric fields at different temperatures (Fig. 11). The "frozen macrodomain" state (FR)

and the "normal ferroelectric" state (FE) are delineated by the boundary line that defines the critical electric field. Both states are bounded at the upper temperature end by the characteristic T_{d0}. At temperatures above T_{d0}, a typical relaxor behavior (R) with polar nanodomains is expected. It is evident from Fig. 11 that the "FE" state in the "PSMN10 ordered" ceramic is shifted to higher temperatures.

Previous studies have shown that both La-doping and Sc-doping are capable of enhancing the B-site cation ordering.[5,9-12,28] However, such enhanced chemical ordering seems to have different effects on the electrical dipole ordering in the polar nanoregions. Such difference may be caused by the different chemical ordering mechanisms. The A-site La-doped PMN takes the chemical formula $Pb_{1-x}La_x(Mg_{(1+x)/3}Nb_{(2-x)/3})O_3$. La^{3+} cation (1.50Å), which has a smaller ionic radius than Pb^{2+} (1.63Å), substitutes Pb cation on the A site sublattice as a donor dopant. The smaller size of the La cation in the A-site and the increased molar fraction of the larger B-site Mg cation are believed to be the primary cause for the enhanced B-site cation ordering.[10,30,31] The smaller La^{3+} also leads to a more compact unit cell which in turn leads to a higher resistance for the shuffling of the ferroelectric active Nb^{5+} in response to external fields. In addition, the increased Mg/Nb ratio in PLMN5 also contributes to the weak ferroelectric response since Mg is ferroelectric inactive.[30,31] Therefore, the field-induced transition to a ferroelectric phase is suppressed in this material.

The ordering mechanism for the Sc-doping is somewhat different. The introduction of larger Sc^{3+} cations (0.885Å) stabilizes the B-site cation order by increasing the size difference between the two B-site sublattices.[30,31] At the same time, the lattice is more open for Nb^{5+} to shuffle in response to external electric fields. In addition, Sc is ferroelectrically more active than

Mg.[31] Therefore, both chemical ordering and electrical dipole ordering are enhanced in the Sc-doped PMN relaxor ferroelectrics.

IV. Conclusions

Both A-site La doping and B-site Sc doping enhance the B-site cation order in PMN-based relaxor ferroelectrics. However, the enhanced chemical ordering has distinct effects on the electrical dipole ordering in these oxides. In the La-doped PMN (PLMN5) ceramic, the dielectric and ferroelectric responses were deeply suppressed. In contrast, the Sc-doped PMN (PSMN5, PSMN10, and "PSMN10 ordered") ceramics display a normal ferroelectric state within a wide temperature range. Both the chemical ordering and the electrical dipole ordering are strengthened at the same time by Sc-doping.

References

[1]G.A. Smolenskii, "Physical phenomena in ferroelectrics with diffused phase transition," *J. Phys. Soc. Japan*, **28**, 26-37 (1970).

[2]L.E. Cross, "Relaxor ferroelectrics," *Ferroelectrics*, **76**, 241-67 (1987).

[3]L.E. Cross, "Relaxor ferroelectrics: An overview," *Ferroelectrics*, **151**, 305-20 (1994).

[4]M.P. Harmer, A. Bhalla, B. Fox, and L.E. Cross, "Electron microscopy of ordered domains in lead scandium tantalate $Pb(Sc_{0.5}Ta_{0.5})O_3$," *Mater. Lett.*, **2**, 278-79 (1984).

[5]J. Chen, H.M. Chan, and M.P. Harmer, "Ordering structure and dielectric properties of undoped and La/Na-doped $Pb(Mg_{1/3}Nb_{2/3})O_3$," *J. Am. Ceram. Soc.*, **72**, 593-98 (1989).

[6]A.D. Hilton, D.J. Barber, C.A. Randall, and T.R. Shrout, "On short range ordering in the perovskite lead magnesium niobate," *J. Mater. Sci.*, **29**, 3461-66 (1990).

[7]M.A. Akbas and P.K. Davies, "Thermally induced coarsening of the chemically ordered domains in $Pb(Mg_{1/3}Nb_{2/3})O_3$ (PMN)-based relaxor ferroelectrics," *J. Am. Ceram. Soc.*, **83**, 119-23 (2000).

[8]G. Burns and F.H. Dacol, "Glassy polarization behavior in ferroelectric compounds $Pb(Mg_{1/3}Nb_{2/3})O_3$ and $Pb(Zn_{1/3}Nb_{2/3})O_3$," *Solid State Comm.*, **48**, 853-56 (1983).

[9]M.A. Akbas, and P.K. Davis, "Domain growth in $Pb(Mg_{1/3}Ta_{2/3})O_3$ perovskite relaxor ferroelectric oxides," *J. Am. Ceram. Soc.*, **80**, 2933-36 (1997).

[10]J.K. Montgomery, M.A. Akbas, and P.K. Davis, "1:1 ordered domain growth in $Pb(Mg_{1/3}Ta_{2/3})O_3$–$La(Mg_{2/3}Ta_{1/3})O_3$," *J. Am. Ceram. Soc.*, **82**, 3481-84 (1999).

[11]L. Farber, M. Valant, M.A. Akbas, and P.K. Davies, "Cation ordering in $Pb(Mg_{1/3}Nb_{2/3})O_3$–$Pb(Sc_{1/2}Nb_{1/2})O_3$ (PMN–PSN) solid solutions," *J. Am. Ceram. Soc.*, **85**, 2319-24 (2002).

[12]L. Farber and P.K. Davies, "Influence of cation order on the dielectric properties of $Pb(Mg_{1/3}Nb_{2/3})O_3$–$Pb(Sc_{1/2}Nb_{1/2})O_3$ (PMN–PSN) relaxor ferroelectrics," *J. Am. Ceram. Soc.*, **86**, 1861-66 (2003).

[13]Y. Yan, S.J. Pennycook, Z. Xu and D. Viehland, "Determination of the ordered structures of $Pb(Mg_{1/3}Nb_{2/3})O_3$ and $Ba(Mg_{1/3}Nb_{2/3})O_3$ by atomic-resolution Z-contrast imaging," *Appl. Phys. Lett.*, **72**, 3145-47 (1998).

[14]Z. Xu, S.M. Gupta, D. Viehland, Y. Yan and S.J. Pennycook, "Direct imaging of atomic ordering in undoped and La-doped $Pb(Mg_{1/3}Nb_{2/3})O_3$," *J. Am. Ceram. Soc.*, **83**, 181-88 (2000).

[15]H. Arndt, F. Sauerbier, G. Schmidt and L.A. Shebanov, "Field-induced phase transitions in $Pb(Mg_{1/3}Nb_{2/3})O_3$ single crystals," *Ferroelectrics*, **79**, 145 (1988).

[16]R. Sommer, N.K. Yushin and J.J. van der Klink, "Polar metastability and an electric-field-induced phase transition in the disordered perovskite $Pb(Mg_{1/3}Nb_{2/3})O_3$," *Phys. Rev. B*, **48**, 13230-37 (1993).

[17]Z.G. Ye and H. Schmid, "Optical, dielectric and polarization studies of the electric field-induced phase transition in $Pb(Mg_{1/3}Nb_{2/3})O_3$ [PMN]," *Ferroelectrics*, **145**, 83-108 (1993).

[18]E.V. Colla, E.Y. Koroleva, N.M. Okuneva and S.B. Vakhrushev, "Long-time relaxation of the dielectric response in lead magnoniobate," *Phys. Rev. Lett.*, **74,** 1681-84 (1995).

[19]Z.G. Ye, "Relaxor ferroelectric $Pb(Mg_{1/3}Nb_{2/3})O_3$: Properties and present understanding," *Ferroelectrics*, **184**, 193-208 (1996).

[20]O. Bidault, M. Licheron, E. Husson and A. Morell, "The onset of an electric field-induced ferroelectric like phase in the perovskite $Pb(Mg_{1/3}Nb_{2/3})O_3$," *J. Phys.: Cond. Matt.*, **8**, 8017-26 (1996).

[21]S.B. Vakhrushev, J.M. Kiat, B. Dkhil, "X-ray study of the kinetics of field induced transition from the glass-like to the ferroelectric phase in lead magnoniobate," *Solid State Comm.*, **103**, 477-82 (1997).

[22]Z.G. Ye, "Relaxor ferroelectric complex perovskites: Structure, properties, and phase transitions," *Key Eng. Mater.*, **155-156**, 81-122 (1998)

[23]B. Dkhil and J.M. Kiat, "Electric-field-induced polarization in the ergodic and nonergodic states of $Pb(Mg_{1/3}Nb_{2/3})O_3$ relaxor," *J. Appl. Phys.*, **90**, 4676-81 (2001).

[24]B.E. Vugmeister and H. Rabitz, "Kinetics of electric-field-induced ferroelectric phase

transitions in relaxor ferroelectrics," *Phys. Rev. B,* **65**, 024111-1 (2002).

[25]Y.J. Chang and Z.L. Chen, "A study of ordered and ferroelectric domains," *Ferroelectrics Lett.*, **4**, 13-18 (1985).

[26]C.A. Randall, D.J. Barber and R.W. Whatmore, "*In situ* TEM experiments on perovskite-structured ferroelectric relaxor materials," *J. Microscopy*, **145**, 275-91 (1987).

[27]S.L. Swartz and T.R. Shrout, "Fabrication of perovskite lead magnesium niobate," *Mater. Res. Bull.*, **17**, 1245-50 (1982).

[28]L.J. Lin and T.B. Wu, "Ordering behavior of lead magnesium niobate ceramics with A-site substitution," *J. Am. Ceram. Soc.*, **73**, 1253-56 (1990).

[29]M.L. Mulvihill, L.E. Cross, W. Cao, and K. Uchino, "Domain-related phase transitionlike behavior in lead zinc niobate relaxor ferroelectric single crystals," *J. Am. Ceram. Soc.*, **80**, 1462-68 (1997).

[30]P.K. Davis and M.A. Akbas, "Chemical order in PMN-related relaxors: structure, stability, modification, and impact on properties," *J. Phys. Chem. Solids*, **61**, 159-66 (2000).

[31]I.W. Chen, "Structural origin of relaxor ferroelectrics—revisited," *J. Phys. Chem. Solids*, **61**, 197-208 (2000).

Fig. 1. SEM micrographs of the fresh fracture surfaces of the four hot-pressed ceramics. (a) PSMN5, (b) PSMN10, (c) PSMN10 ordered, and (d) PLMN5.

Fig. 2. X-ray diffraction spectra of the PSMN5, PSMN10, PSMN10 ordered, and PLMN5 ceramics. The 1:1 cation order is detected in the "PSMN10 ordered" and PLMN5 ceramics.

Fig. 3. TEM dark field imaging with the (½ ½ ½) superlattice spot in the <110>-zone axis electron diffraction pattern. (a) PSMN10 ordered, and (b) PLMN5.

Fig. 4. Dielectric properties of the PSMN5, PSMN10, "PSMN10 ordered", and PLMN5 ceramics. (a) Relative permittivity vs. temperature plot at 1kHz, 10kHz, and 100kHz. (b) Dielectric loss vs. temperature plot at 1kHz, 10kHz, and 100kHz.

Fig. 5. Depolarization current measurement under zero-field heating of the hot-pressed ceramics after field-cooling at 10kV/cm.

Fig. 6. Polarization vs. electric field curves measured at 4 Hz with the PLMN5 ceramic at (a) -100°C, (b) -120°C, (c) -150°C, and (d) -196°C.

Fig. 7. Polarization vs. electric field curves measured at 4 Hz at -50°C, -80°C, -120°C, and -150°C, respectively. (a) PSMN5, (b) PSMN10, (c) PSMN10 ordered.

Fig. 8. Ferroelectric properties of the four ceramics measured from the P~E hysteresis loops. (a) Remanent polarization P_r, and (b) coercive field E_c.

Fig. 9. History dependence of the ferroelectric behavior in the relaxor ferroelectric PSMN10 ceramic. ○: the "zero-field cooled" condition; ●: the "poled" condition. (a) 15kV/cm at -120°C, (b) 20kV/cm at -120°C, (c) 10kV/cm at -100°C, and (d) 5kV/cm at -80°C.

Fig. 10. History dependence of the ferroelectric behavior in the relaxor ferroelectric “PSMN10 ordered” ceramic. ○: the “zero-field cooled” condition; ●: the “poled” condition. (a) 19kV/cm at -120°C, (b) 10kV/cm at -80°C, and (c) 5kV/cm at -50°C.

Fig. 11. The electric field-temperature phase diagram proposed for the relaxor ferroelectric PSMN10 and “PSMN10 ordered” ceramics based on the history dependence. “R” denotes the relaxor ferroelectric nanodomain state, “FE” denotes the normal ferroelectric macrodomain state, and “FR” denotes the frozen ferroelectric macrodomain state.

Table 1. Dielectric properties of the Sc-doped and La-doped PMN ceramics.

Ceramic	$\varepsilon_{r,max}$ @ 1kHz	Peak loss @ 1kHz	T_{max} @ 1kHz (°C)	T_{d0} (°C)
PSMN5	19674	0.105	-12	-66
PSMN10	17518	0.115	-8	-64
PSMN10 ordered	15436	0.116	-17	-51
PLMN5	3245	0.102	-80	-155

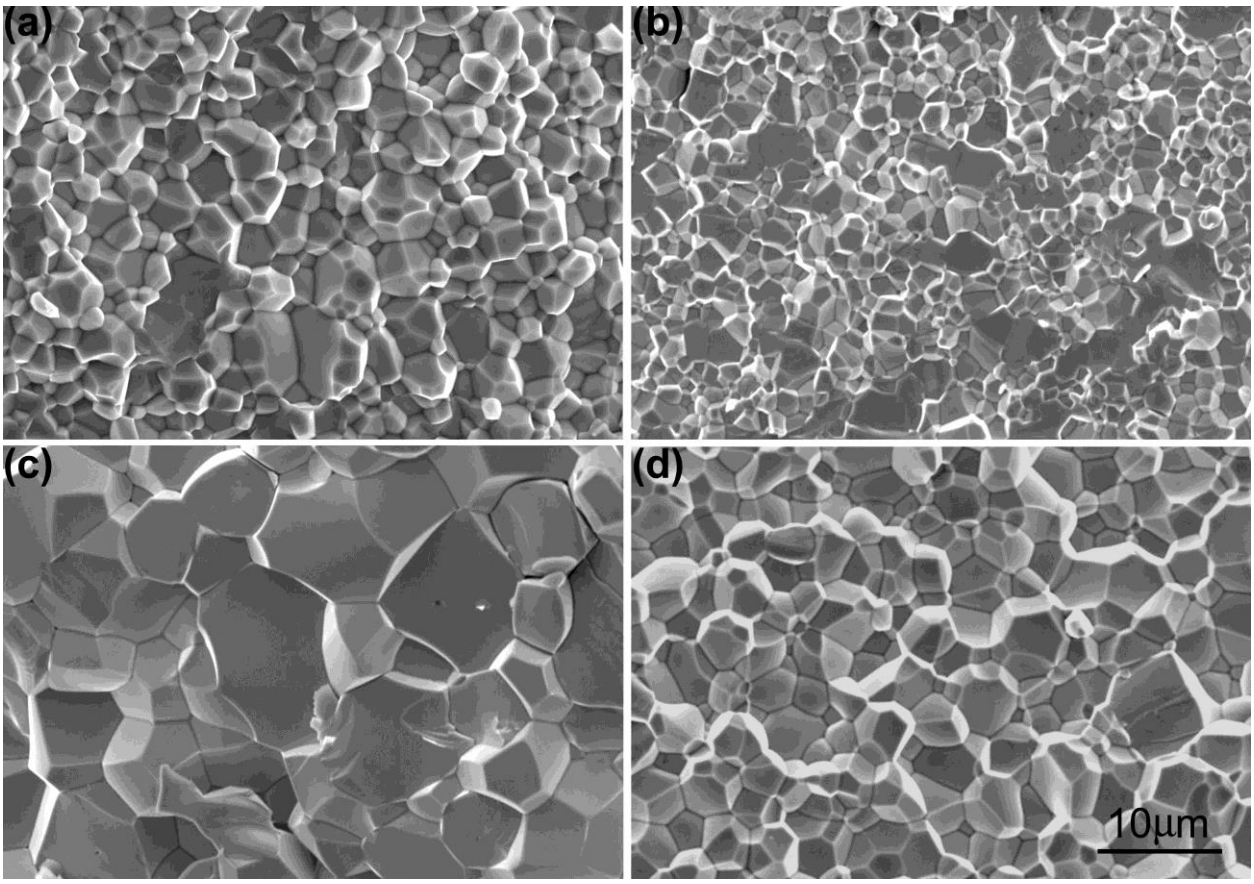

Fig. 1

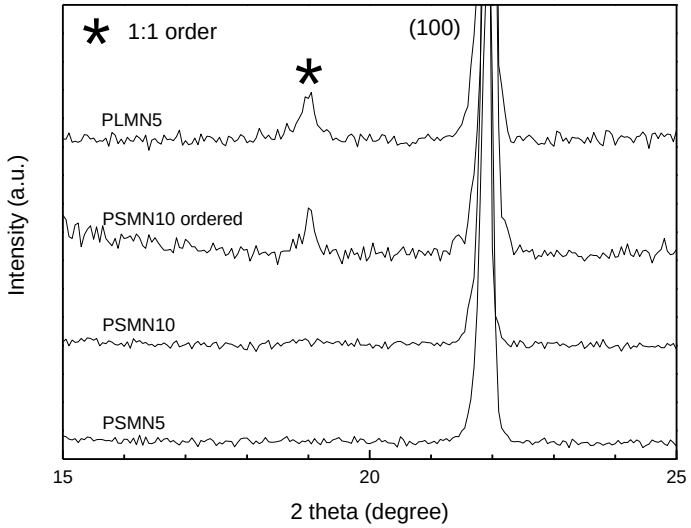
* 1:1 order
(100)
*
PLMN5
PSMN10 ordered
PSMN10
PSMN5
Intensity (a.u.)
15
20
25
2 theta (degree)

Fig. 2

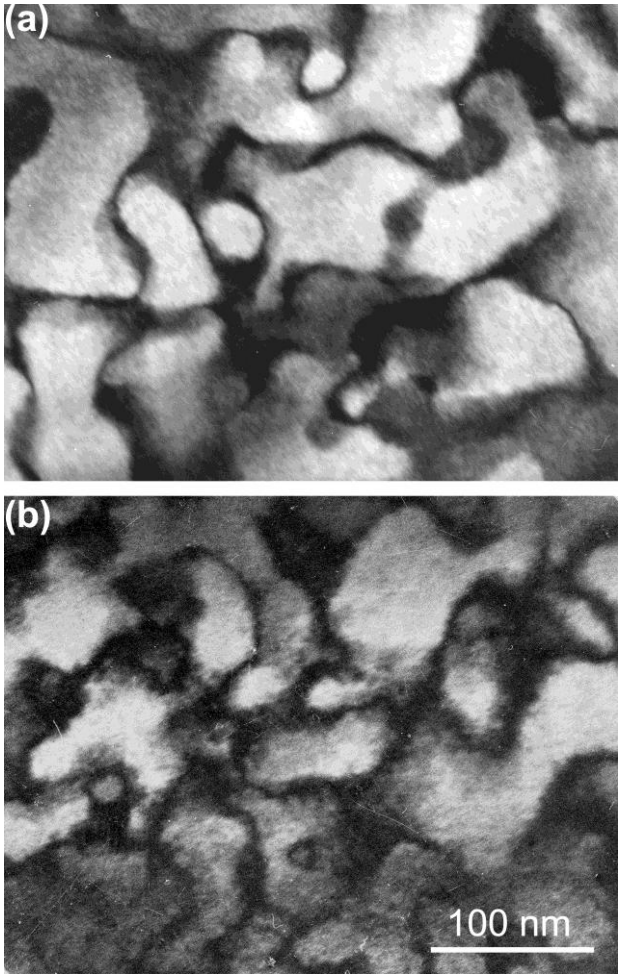

Fig. 3

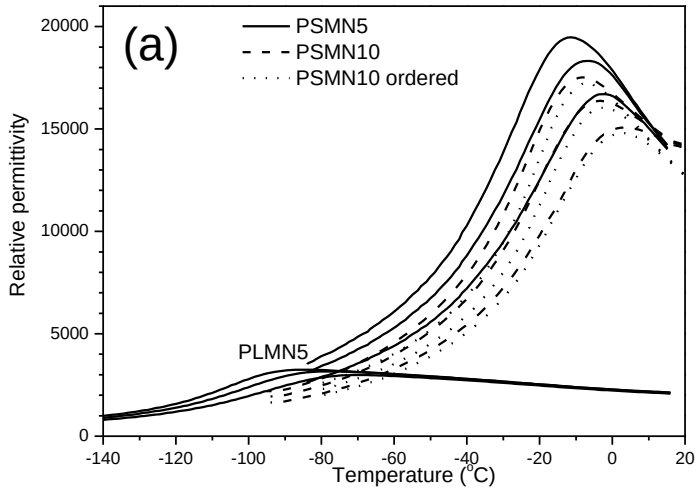
(a)
PSMN5
PSMN10
PSMN10 ordered
PLMN5
Relative permittivity
Temperature (°C)
20000
15000
10000
5000
0
-140
-120
-100
-80
-60
-40
-20
0
20

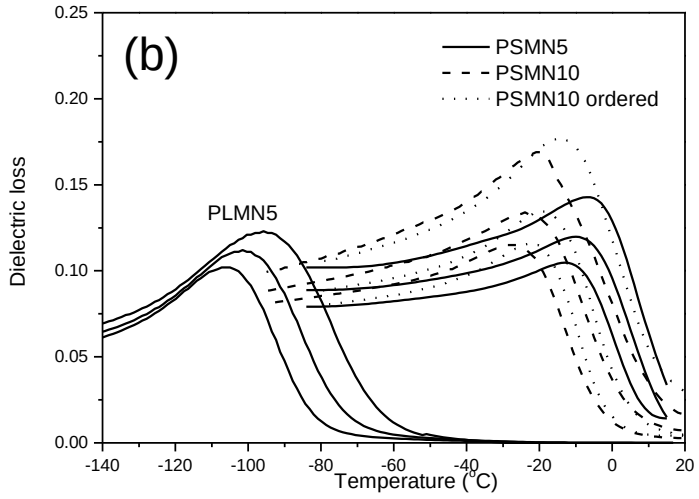
(b)
PSMN5
PSMN10
PSMN10 ordered
PLMN5
Dielectric loss
Temperature (°C)
0.25
0.20
0.15
0.10
0.05
0.00
-140
-120
-100
-80
-60
-40
-20
0
20

Fig. 4

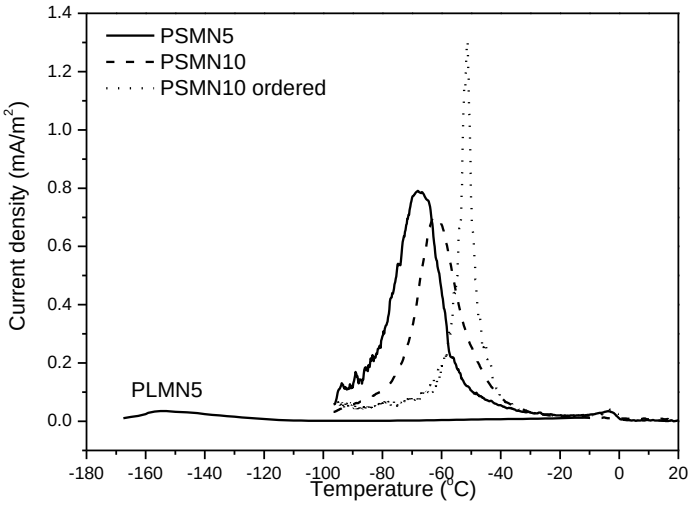
PSMN5
PSMN10
PSMN10 ordered
PLMN5
Current density (mA/m^2)
Temperature (^{o}C)
1.4
1.2
1.0
0.8
0.6
0.4
0.2
0.0
-180
-160
-140
-120
-100
-80
-60
-40
-20
0
20

Fig. 5

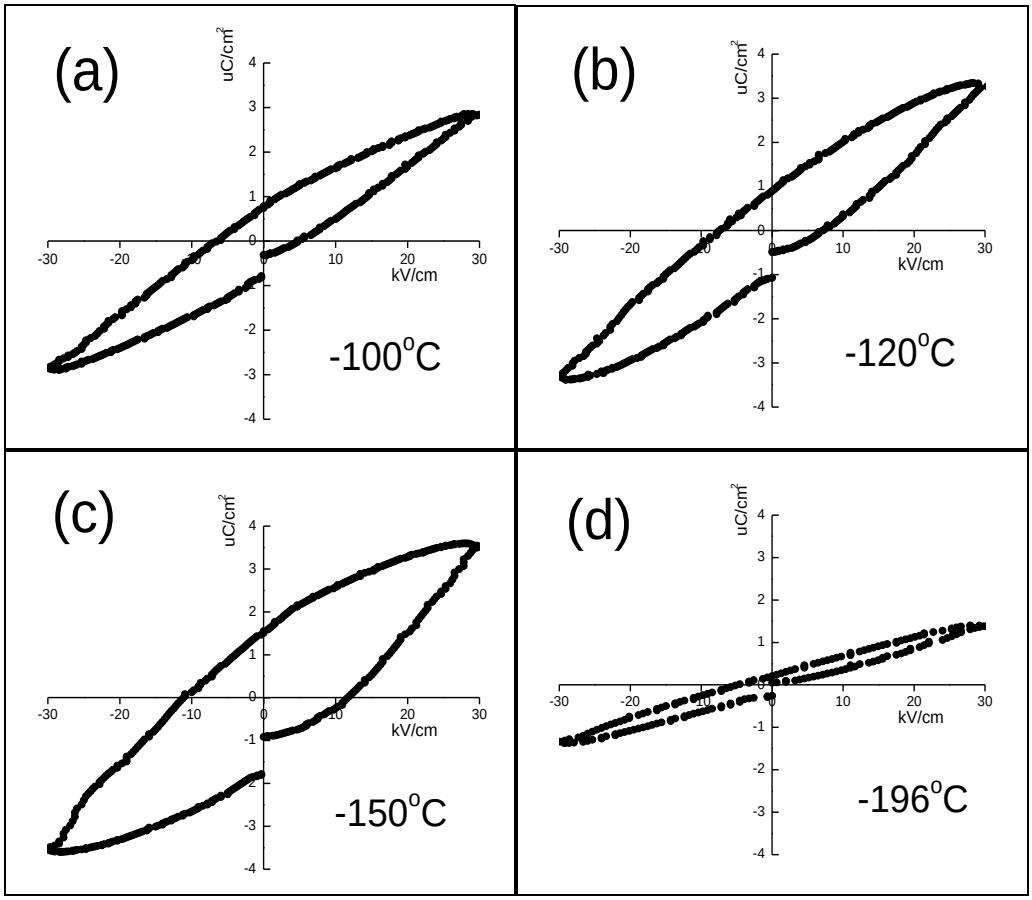
(a)
uC/cm2
kV/cm
-100°C
(b)
uC/cm2
kV/cm
-120°C
(c)
uC/cm2
kV/cm
-150°C
(d)
uC/cm2
kV/cm
-196°C

Fig. 6

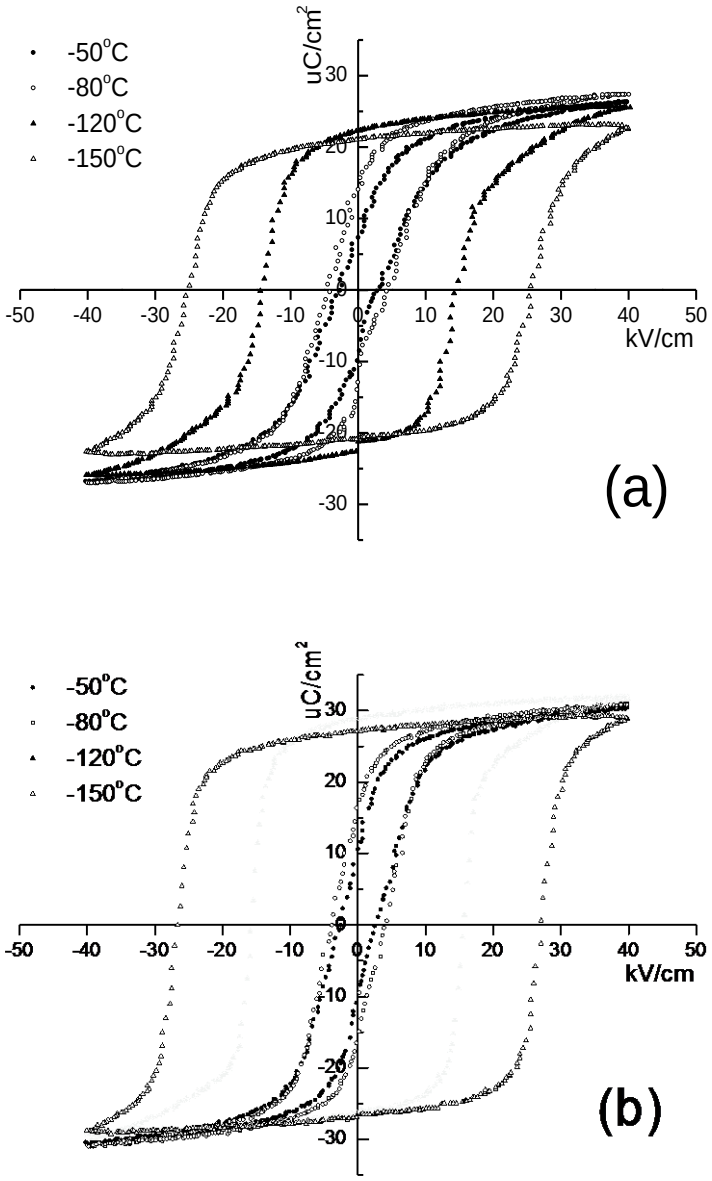

Fig. 7 (a), (b)

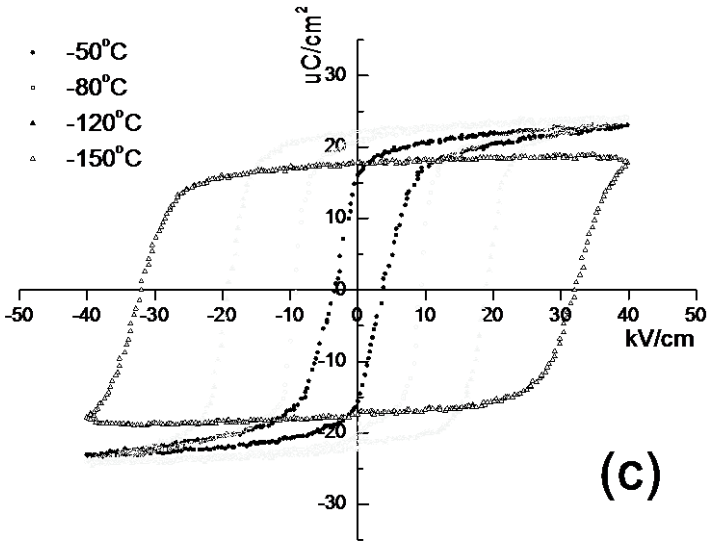
-50°C
-80°C
-120°C
-150°C
uC/cm²
30
20
10
0
-10
-20
-30
-50
-40
-30
-20
-10
0
10
20
30
40
50
kV/cm
(c)

Fig. 7(c)

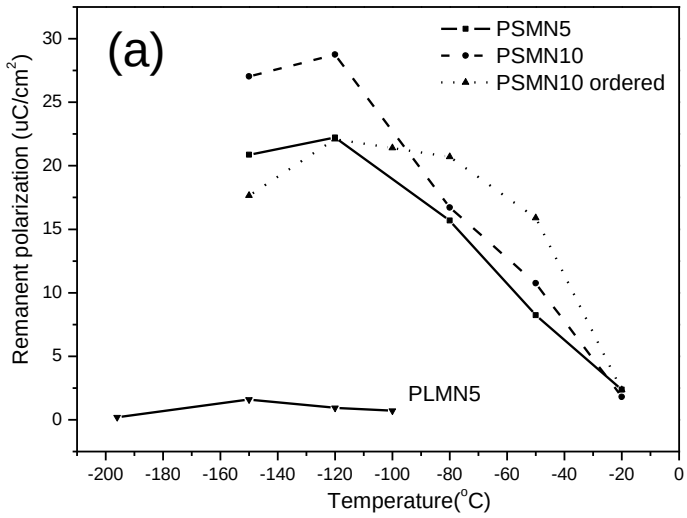
(a)
PSMN5
PSMN10
PSMN10 ordered
PLMN5
Remanent polarization (uC/cm^2)
Temperature(^{o}C)
30
25
20
15
10
5
0
-200
-180
-160
-140
-120
-100
-80
-60
-40
-20
0

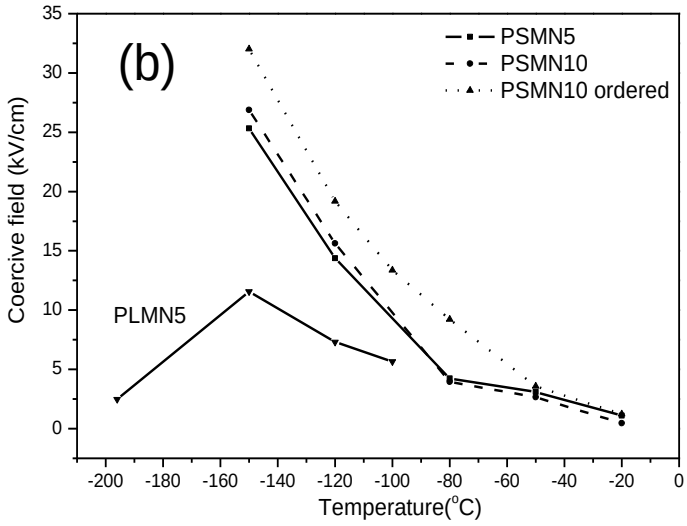
(b)
PSMN5
PSMN10
PSMN10 ordered
PLMN5
Coercive field (kV/cm)
Temperature(^{o}C)
35
30
25
20
15
10
5
0
-200
-180
-160
-140
-120
-100
-80
-60
-40
-20
0

Fig. 8

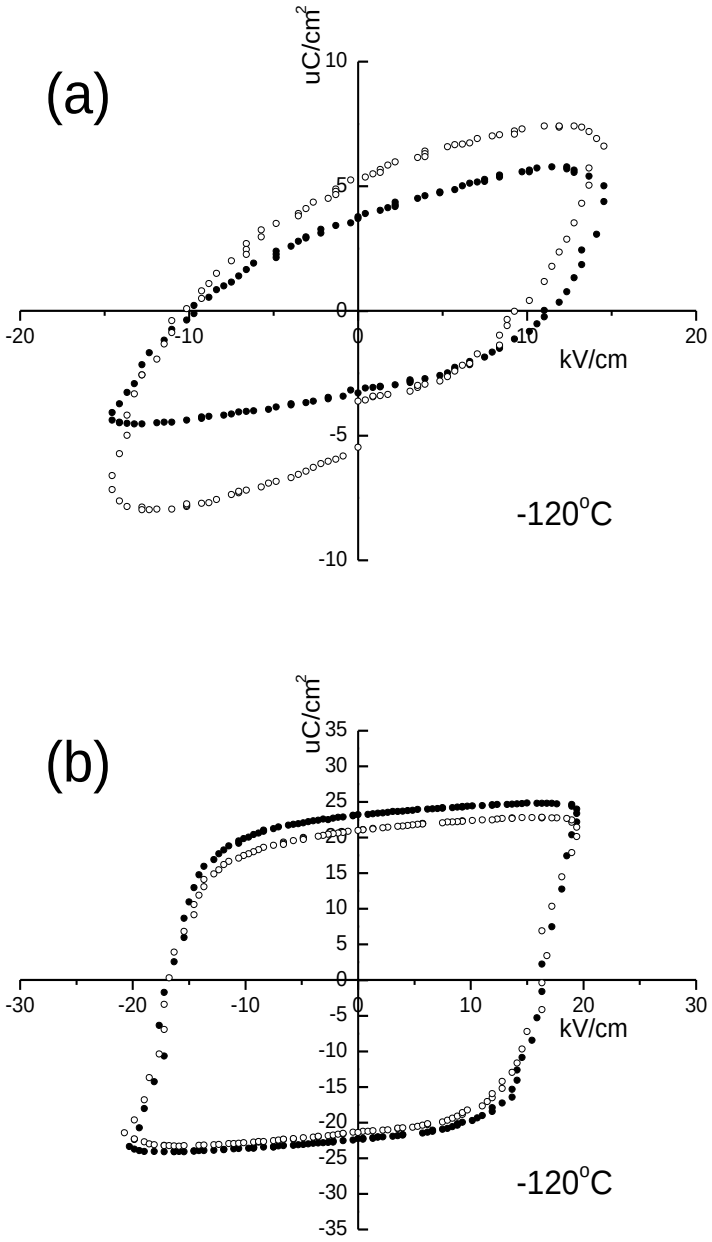
(a)
uC/cm2
10
5
0
-5
-10
-20
-10
0
10
20
kV/cm
-120°C
(b)
uC/cm2
35
30
25
20
15
10
5
0
-5
-10
-15
-20
-25
-30
-35
-30
-20
-10
0
10
20
30
kV/cm
-120°C

Fig. 9 (a), (b)

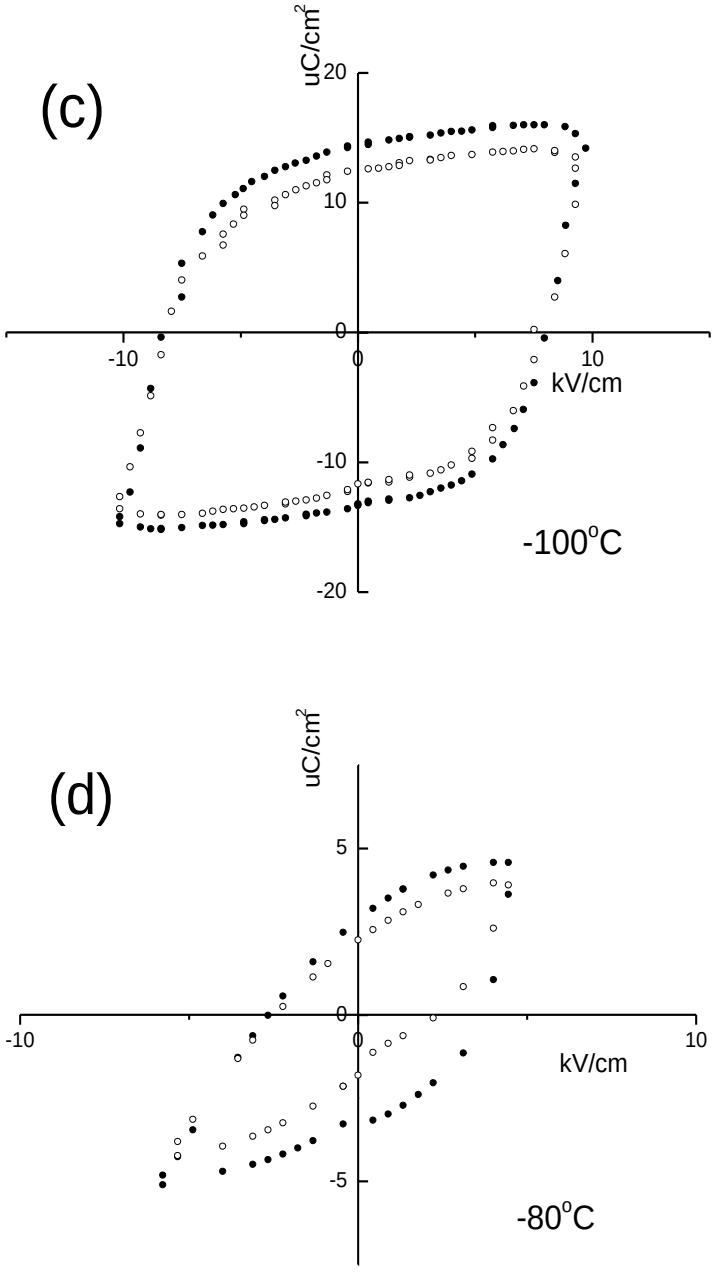

Fig. 9 (c), (d)

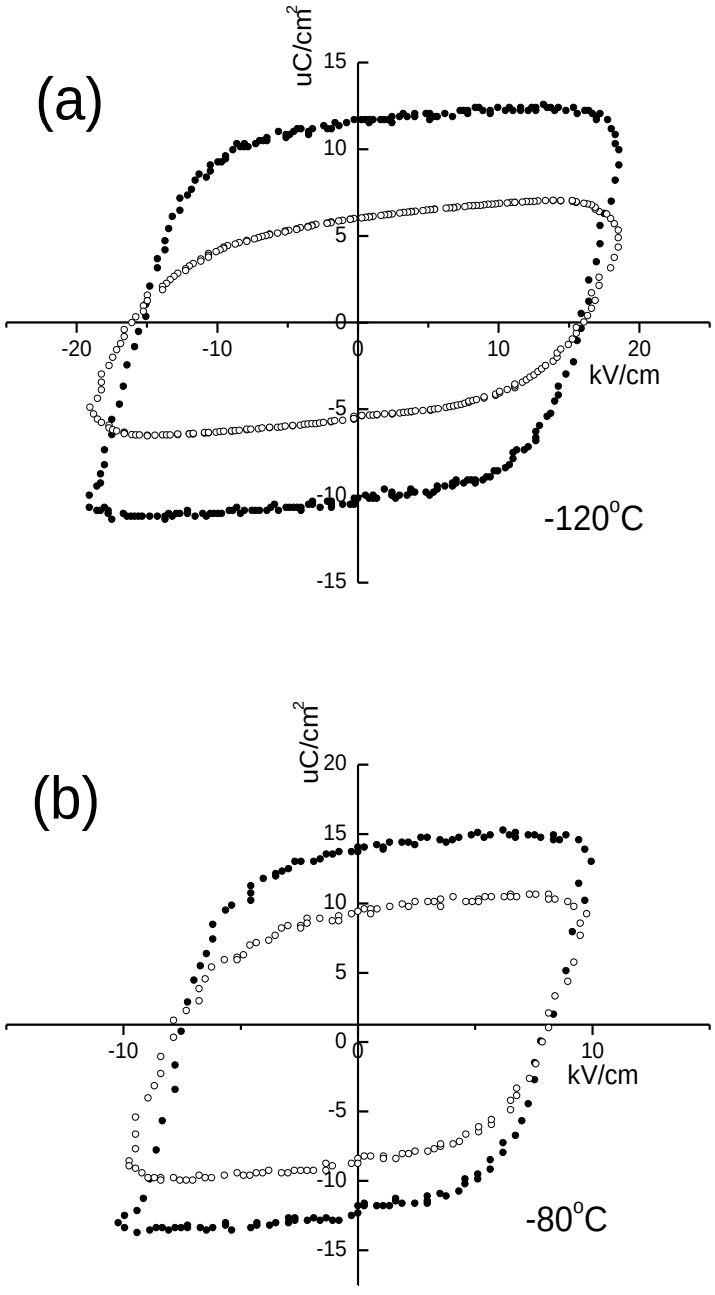
(a)
uC/cm2
15
10
5
0
-5
-10
-15
-20
-10
0
10
20
kV/cm
-120°C
(b)
uC/cm2
20
15
10
5
0
-5
-10
-15
-10
0
10
kV/cm
-80°C

Fig. 10 (a), (b)

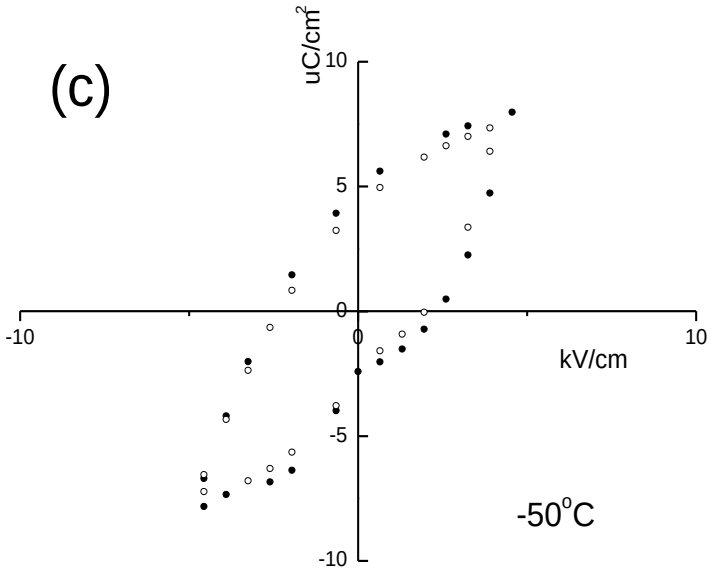

Fig. 10(c)

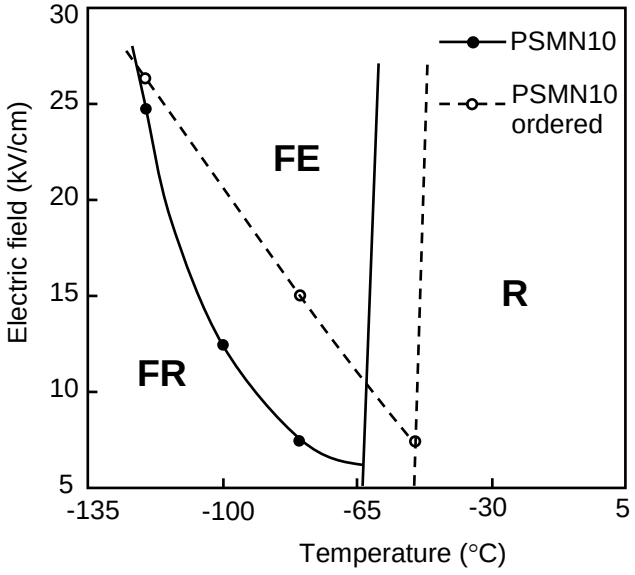
30
25
20
15
10
5
Electric field (kV/cm)
-135
-100
-65
-30
5
Temperature (°C)
PSMN10
PSMN10
ordered
FE
R
FR

Fig. 11